Jurnal
Teknologi

Full Paper

# INTEGRATED HIGH MAGNETIC GRADIENT SYSTEM FOR TRAPPING NANOPARTICLES

Ummikalsom Abidin,[a,b,*] Burhanuddin Yeop Majlis,[b] Jumril Yunas,[b]

[a]Faculty of Mechanical Engineering, Universiti Teknologi Malaysia, 81310 UTM Johor Bahru, Johor, Malaysia
[b]Institute of Microengineering and Nanoelectronics (IMEN), Universiti Kebangsaan Malaysia, 43600 UKM Bangi, Selangor, Malaysia

**Article history**
Received
*20 February 2015*
Received in revised form
*19 March 2015*
Accepted
*27 March 2015*

*Corresponding author
ummi@fkm.utm.my

## Graphical abstract

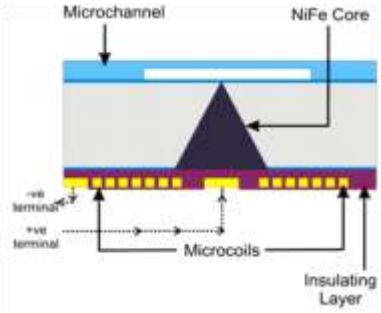


## Abstract

Lab-on-chip (LoC) magnetic separator is important in clinical diagnostics and biological studies where different types of biological cells need to be isolated from its heterogeneous population. In this work, a novel design of on-chip V-shaped magnetic core generating high magnetic gradient and force for trapping magnetically labelled bioparticles is presented. The integrated magnetic system consisted of a spiral-shaped planar microcoils and a V-shaped permalloy ($Ni_{80}Fe_{20}$) magnetic core structure, which was designed to be part of LoC separator system. The effects of V-shaped magnetic core tip area, the current injection to the microcoils on the magnetic field, as well as its gradient and force on magnetic nanoparticles were simulated and analyzed. Finite element analysis (FEA) simulation using two dimensional (2D) axial symmetry model and steady state analysis of the DC magnetostatics module confirmed the effect of V-shaped magnetic core tip on the high magnetic field generation. The smallest V-shaped magnetic core tip area and the highest current injected to the magnetic coils had significantly amplified the magnetic flux density, its gradient, and the magnetic force generated on a magnetic nanoparticles. Functional test results justified the proportional relationship between DC applied and the trapping area of the magnetic nanoparticles. Effective separation of biological cells tagged with magnetic nanoparticles in LoC system was expected with integration of this high gradient on-chip magnetic system.

*Keywords*: V-shaped magnetic core; Lab-on-chip (LoC); high magnetic gradient; bioparticles; microfluidics; nanoparticles

## Abstrak

Pemisah magnetik makmal-atas-chip (LoC) adalah penting bagi bidang diagnostik klinikal dan biologi bagi mengasingan sel biologi yang berbeza daripada populasi heterogennya. Sistem magnetik ini mengintegrasi komponen gegelung lingkaran satah mikro dan teras berbentuk-V *permalloy* ($Ni_{80}Fe_{20}$) yang direka sebagai sebahagian daripada sistem pemisah LOC. Kesan luas hujung teras berbentuk-V, arus terus bekalan terhadap medan magnet, kecerunannya, dan daya ke atas partikel bersaiz nano telah disimulasi dan dianalisis. Medan magnet, kecerunan, dan daya magnetik ke atas partikel nano yang lebih lebih kuat dapat dihasilkan dengan hujung teras yang kecil dan arus terus bekalan yang besar. Ujian fungsi pemerangkapan menjustifikasi hubungan perkadaran antara arus terus DC dan luas pemerangkapan partikel magnetik bersaiz nano.

*Kata kunci*: Teras magnetik berbentuk-V; makmal-atas-cip (LOC); kecerunan magnetik tinggi; mikrofluidik, partikel nano

© 2015 Penerbit UTM Press. All rights reserved

## 1.0 INTRODUCTION

Clinical diagnostics and cell biology studies require bioparticles, i.e. viruses, bacteria, and cancer cells separation from human fluid sample. In recent years, research and development of Lab-on-chip (LoC) device for bioparticles separation have increased significantly. Some of the advantages of LoC are it reduces sample volume needed, has fast reaction time, high throughput, systems compactness, and lower fabrication possibility [1]. LoC magnetic separator utilizes continuous microfluidics channel flow, external magnetic field generator, and superparamagnetic nanoparticles (SPION) or magnetic microbeads. The SPION used in LoC devices can be in the form of ferrofluid, where 50 to 500 nm size particles are embedded within dextran and magnetic microbeads in the range of 500 nm to 10 µm size within polystyrene or silica microspheres [2]. The volume, magnetic susceptibility, and surface functionality of the SPION and magnetic beads make it possible to be used in tagging as well as further trapping and separating a wide range of bioparticles, i.e. cell of 10 – 100 $\mu$m, virus of 20 – 450 nm, and protein of 5 – 50 nm from the biological fluid sample [3].

High magnetic field and its gradient generation are important in offering high magnetic force on trapping and separating bioparticles. To date, permanent magnet, microelectromagnet, and the hybrid system of both have been used as magnetic bioparticles separator [4]. High magnetic field is possible to be generated from a permanent magnet. However, it bulkiness, incapable for field tuning and poor magnetic flux density gradient, inhibit its usage in LoC applications. Microelectromagnet is possible to be integrated as part of LoC system via microfabrication technology. Besides, microelectromagnet of different designs and structures generate high magnetic field and its gradient has been studied as part of LoC device [5]–[10]. Integration of magnetic materials, i.e. permalloy and nickel, has also been used with either external permanent or electromagnet in enhancing the magnetic field gradient [11]–[13]. High magnetic field and its gradient are generated by spiral- and square-shaped planar microcoils due to the summation of total magnetic flux density at its center. In addition, a high magnetic gradient is possible to be generated from a wire wound around a tapered core structure or a needle tip [14]–[16].

This paper studied the effect of V-shaped magnetic core of micron-size tip in generating high magnetic force on a magnetic particle. The integrated magnetic sensor elements consisted of spiral-shaped planar microcoils and a V-shaped nickel iron ($Ni_{80}Fe_{20}$) or permalloy magnetic core structure. Besides, finite element analysis (FEA) of the integrated micro-electromagnet system was conducted in determining the magnetic flux density and its gradient value. Furthermore, the effect of the V-shaped core magnetic tip area, injected current to the microcoils, effect of height above the core tip on the magnetic field, and force generated are presented. Effective trapping of bioparticles tagged with SPION for LOC application was expected with this simple and novel magnetic system.

## 2.0 THEORETICAL

### 2.1 Magnetic Force on a Magnetic Particle

In trapping bioparticles tagged with magnetic nano or microparticles, an inhomogeneous magnetic field of high gradient is required [17]. This high magnetic flux density gradient is possible to be generated with a combination of soft magnetic materials structure, i.e. core and pillars. Furthermore, soft magnetic materials of high permeability are able to direct the magnetic field line from the magnet source. The principle of the magnetic separation of magnetic particles in the continuous microfluidics flow involves the interaction of magnetic and hydrodynamics forces. The magnetic force, $F_m$, developed on a magnetic particle of volume, $V=(4/3)\pi r^3$, with different magnetic susceptibility, $\Delta\chi$, ($\chi_p$ for particle and $\chi_m$ for the buffer medium), as well as the strength and the gradient of the magnetic flux, density $B$ can be theoretically calculated as [18]:

$$\vec{F}_m = \frac{V\Delta\chi}{\mu_0}(\vec{B}\cdot\vec{\nabla})\vec{B} = \frac{V\Delta\chi}{2\mu_0}\vec{\nabla}(\vec{B}\cdot\vec{B}) \quad (1)$$

where, $\mu_0$ is the permeability of free space, which is $4\pi$ x $10^{-7}$ H/m. In the real system, where the magnetic susceptibility of the buffer medium is in the range of $10^{-6}$, the particle magnetic susceptibility is used. In the direction of flow, the x-component of the force on the magnetic particles can be written as

$$F_{m,x} = \frac{V\Delta\chi}{\mu_0}\left(B_x\frac{\partial}{\partial x} + B_y\frac{\partial}{\partial y} + B_z\frac{\partial}{\partial z}\right)B_x \quad (2)$$

In two dimensional (2D) axial symmetrical configuration, the magnetic force along the radial axis becomes

$$F_{m,r} = \frac{V\Delta\chi}{\mu_0}\left(B_r\frac{\partial B_r}{\partial r} + B_z\frac{\partial B_r}{\partial z}\right) \quad (3)$$

A magnetic particle of radius, $R$, experiences hydrodynamics drag force in the microfluidics channel flow. According to Stoke's Theorem, the drag force, $F_d$ is

$$\vec{F}_d = 6\pi\eta R\left(v_p - v_{medium}\right) \quad (4)$$

where $v_p$ is the particles velocity, $v_{medium}$ is the fluid velocity, and $\eta$ is the fluid viscosity. In order to

successfully trap the magnetic particles in the continuous microfluidics channel flow, the magnetic force must be greater in comparison to the drag force experienced by the magnetic particle.

$$\vec{F}_m > \vec{F}_d \quad (5)$$

## 3.0 METHODOLOGY

### 3.1 Design Of The Integrated Magnetic System

In this work, a novel design of the on-chip magnetic system was proposed. The integrated magnetic system was made up of copper planar microcoils as a magnetic field source and silicon-based V-shaped structure permalloy magnetic core as the magnetic concentrator. The high magnetic flux density gradient was generated by the magnetic core and exerted in capturing the magnetic force on the magnetic nanoparticles. On top of that, silicon of high thermal conductivity and low thermal expansion coefficient were used in minimizing the Joule heating effect from the microcoils. Furthermore, the V-shaped silicon cavity structure was fabricated via anisotropic etching of potassium hydroxide (KOH) on the silicon (100) silicon. The V-shaped cavity structure was then filled with permalloy materials of high magnetic saturation and permeability using electroplating process. The microcoils were fabricated by etching the deposited copper layer on the silicon substrate. For a complete LoC device, a microfluidic channel was integrated to the magnetic sensor system. The proposed integrated device is depicted in Figure 2.

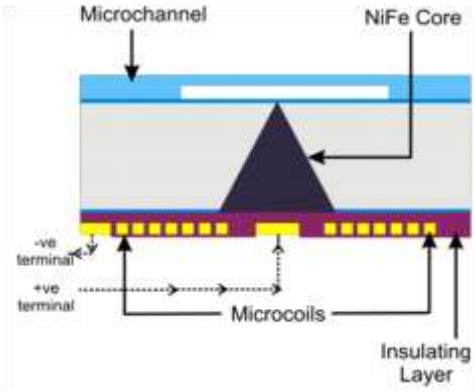


**Figure 1** (a) Schematic 2D view of the proposed magnetic system of microcoils, V-shaped permalloy core, and microfluidic channel

### 3.2 DC Magnetostatics of 2D Axial Symmetry Model

In this work, Finite Element Analysis (FEA) was used to model and to simulate the proposed design in obtaining the magnetic flux density and its gradient. In the simulation, the DC magnetostatics module of current carrying conductor was used. The permalloy magnetic material used was considered linear and isotropic with relative permeability value of 3000 [19]. Besides, air and other non-magnetic materials used in this study had 1 as the relative permeability value. In this FEA simulation, the magnetic fields interface was used. In obtaining the magnetic vector potential, the Ampere's Law was solved by the magnetic fields interface [20]. The mesh set for this analysis was physics-control mesh of extremely fine.

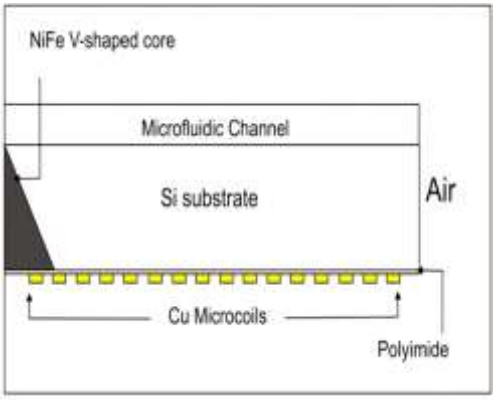


**Figure 2** Magnetic system model used for the Finite Element Analysis (FEA)

In order to reduce the computational time and to solve complexity, a simplification of the three-dimensional (3D) model to two-dimensional (2D) axial symmetry geometry model was made [19]. The 2D axial symmetry model is shown in Fig. 3, while Table 1 lists the geometrical parameters used in the design and simulation model. In this 2D axial symmetry model, tip radius of 0.56, 1.13, 2.26, 2.82, 5.64, 16.93, and 27.37 μm were used to correspond to the tip area size of 1, 4, 25, 100, 900, and 2353 μm$^2$ respectively. The direct current, $I_{DC}$ used had been 0.5, 1.0, 2.0, and 3.0 Ampere (A).

**Table 1** Geometrical parameters used in designing and modelling

| Geometrical Parameters | | Value | Unit |
|---|---|---|---|
| **Substrate** | Si | | |
| Thickness | $t$ | 670 | μm |
| **Microcoil** | Cu | | |
| Width | $w$ | 50 | μm |
| Spacing | $s$ | 50 | μm |
| Thickness | $t$ | 5 | μm |
| Outer radius | $r_o$ | 1300 | μm |
| Winding | $N$ | 10 | |
| **Magnetic Core** | NiFe | | |
| Tip surface area | $A$ | varied | μm$^2$ |
| Height | $h$ | 670 | μm |

In this simulation work, the parametric sweep of the V-shaped core tip area and the *DC* current were performed. The magnetic flux density and its gradient data were generated from the simulation result after

the convergence solution was accomplished by the solver. The magnetic force developed on different diameter magnetic nanoparticles was calculated from equations (2) and (3) using the simulated magnetic flux density and its gradient values.

### 3.3 Magnetic Core Functional Test

In the magnetic core functional testing, the magnet wire coil was connected to DC power supply (ISO-TECH IPS 3202, Texas Instruments, USA) in supplying the magnetic field source. The DC current was controlled by manually setting the fixed current value to be used. The magnetic flux density on the magnetic core was measured by using a portable gauss meter (MAGSYS Magnet System, Germany) of model HGMO9 with a standard transversal probe. The magnetic flux density on the magnet wire coil had been 0.65 mT, 1.29 mT, 2.59 mT, and 3.89 mT at DC of 0.5 A, 1.0 A, 2.0 A, and 3.0 A respectively. The magnet wire coil was used as a groundwork solution for the V-shaped magnetic core functional test. The magnetic core size area used in this testing was ~ 2353 $\mu m^2$. A digital camera connected to the optical microscope (Olympus, Germany) and the image analyzer using Analysis software had been then synchronized. Besides, focusing on the trapping area on the V-shaped magnetic tip was conducted to give an overall picture of the capturing area. Nickel passivated nanoparticles (Nanostructured and Amorphous Materials, USA) with an average size of 20 nm was mixed with deionized water prior to the magnetic device function test was conducted. The details of the properties of the nickel nanoparticles used are listed in Table 2. The nanoparticles solution in deionized (DI) mixture was dispensed onto the core tip at 10 μL volume using adjustable micropipette.

**Table 2** Nickel-passivated nanoparticles properties

| Specification | Value |
|---|---|
| Purity | > 99.9% (metal basis) |
| Composition | O < 10 % |
| Average Nanoparticle Size | 20 nm |
| Specific Surface Area | 40-60 $m^2/g$ |
| Nanoparticle Morphology | spherical |
| Crystallographic Structure | cubic |
| Melting Point | 1453 °C |
| Boiling Point | 2730 °C |
| Density | 8.908 g/cm3 |
| CAS No. | 7440-02-0 |

## 4.0 RESULTS AND DISCUSSION

### 4.2 Magnetic Flux Density Generation

This section discusses the magnetic flux density generated and the magnetic force developed on a nanoparticle from the proposed V-shaped magnetic core and microcoils system. The *r*-coordinate is the radial distance and the z-coordinate is the axis that is perpendicular to the axis of the channel. Z-coordinate of z = 0 corresponded to the distance just above the V-shaped core tip. As the basis of this study, a simulation of spiral planar microcoils of 10 turns without core integration was also performed. The highest magnetic flux density of the spiral microcoils was at the center due to the summation of the magnetic field from each individual coil, as shown in Figure 3. The highest magnetic flux density value of these spiral microcoils was 76.6 mT at $I_{dc}$ = 3.0 A. Theoretically, high magnetic permeability core can guide, concentrate, and intensify the magnetic potential generated by solenoids or coils. From the FEA analysis, it had been confirmed that the V-shaped magnetic core had significantly increased the magnetic flux density generation. The magnetic flux density generated in 2D contour plot for $I_{dc}$ of 3.0 A with tip area of 2363 $\mu m^2$ is depicted in Figure 4. The highest magnetic flux density value was 144.9 mT. Besides, permalloy core of a permeable ferromagnetic material resulted in ease of magnetic flux lines path due to its low reluctance [5]. The close-up value of the magnetic core tip contour plot is illustrated in Figure 5. The contour plot also represents the gradient change of the magnetic flux density. The greater the distance above the core tip, the less the magnetic flux density gradient. Moreover, the greatest magnetic flux density gradient was observed at the corner of the tip core due to the highest intensity of the magnetic flux lines.

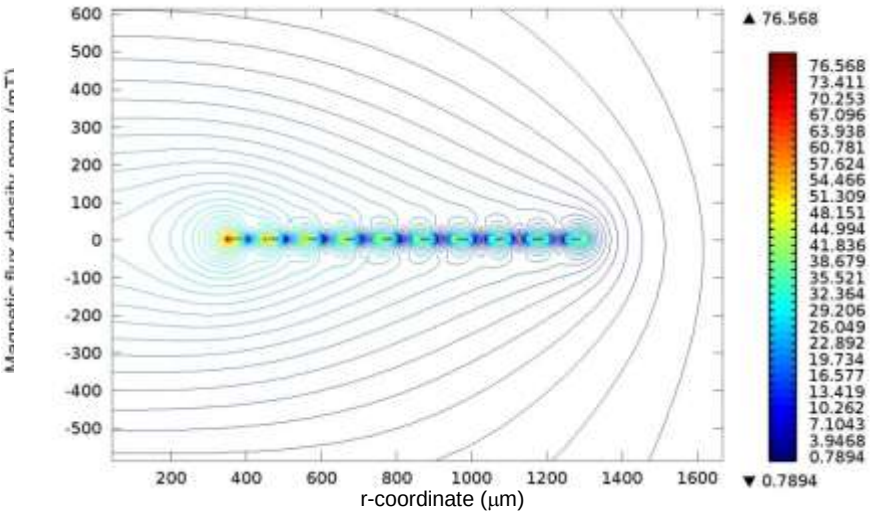


**Figure 3** 2D contour plot of the normal magnetic flux density, $B_{norm}$ from $N$ = 10 microcoils

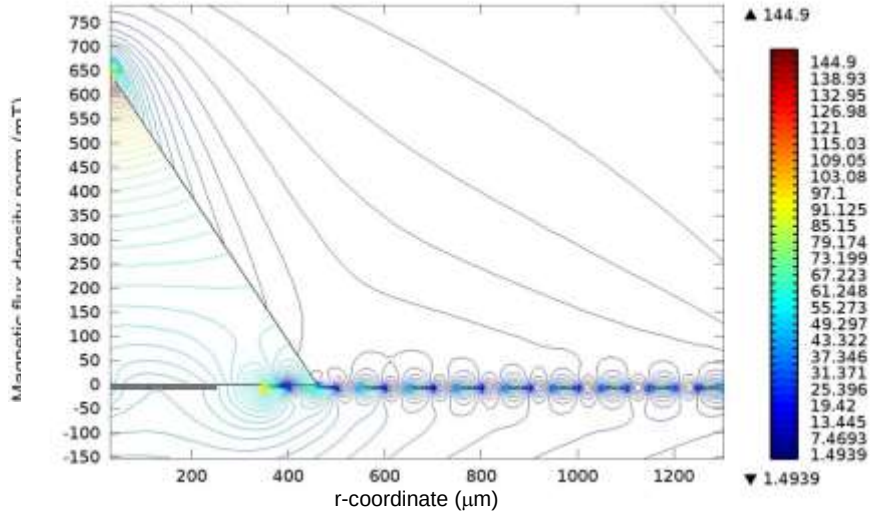


**Figure 4** 2D contour plot of the normal magnetic flux density, $B_{norm}$ from magnetic system of $N$ = 10 microcoils, and V-shaped core tip of 2353 μm$^2$

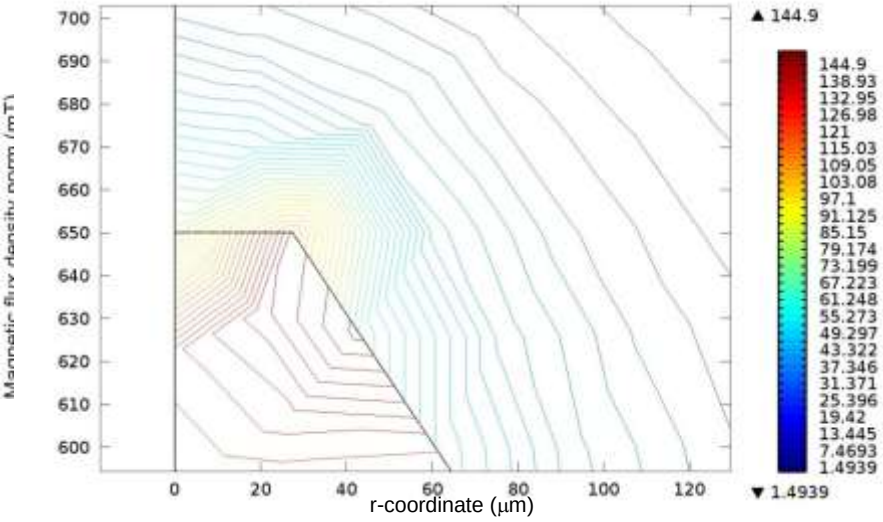


**Figure 5** Close-up view of the 2D contour plot of the normal magnetic flux density, $B_{norm}$ from magnetic system of $N$ = 10 microcoils, and V-shaped core tip of 2353 μm$^2$

### 4.2 Effect Of V-Shaped Magnetic Core Tip Area On Magnetic Flux Density And Its Gradient

At a very small V-shaped magnetic core tip area, considerable high values of $B_{norm}$ and its gradient were obtained, which corresponded to tip areas 1, 4, and 16 μm$^2$. However, a gradual drop of maximum $B_{norm}$ and their gradients were observed at tip areas of 25, 100, 900, and 2353 μm$^2$. The $B_{norm}$ profiles with tip area variations for $I_{dc}$ = 1.0 A and $I_{dc}$ = 3.0 A are shown in Figures 6 and 7 respectively. The gradient values of the V-shaped core tip could be observed from the potential well created. The steep potential well corresponded to the small core tip area of a small radius. This localized high gradient area resulted in magnetic particles trapping concentration in an actual experiment [12]. The smallest magnetic core tip area and the highest current injection to the magnetic system resulted in the highest magnetic flux density and its gradient value. In this work, V-shaped core tip of 1 μm$^2$ generated magnetic flux density of 1300 mT and 440 mT at $I_{dc}$ = 3.0 A and $I_{dc}$ = 1.0 A respectively. In comparison to spiral microcoils of no core, an approximately seventeen times greater magnetic flux value was obtained with V-shaped magnetic core of 1 μm$^2$ tip at the same injected current magnitude.

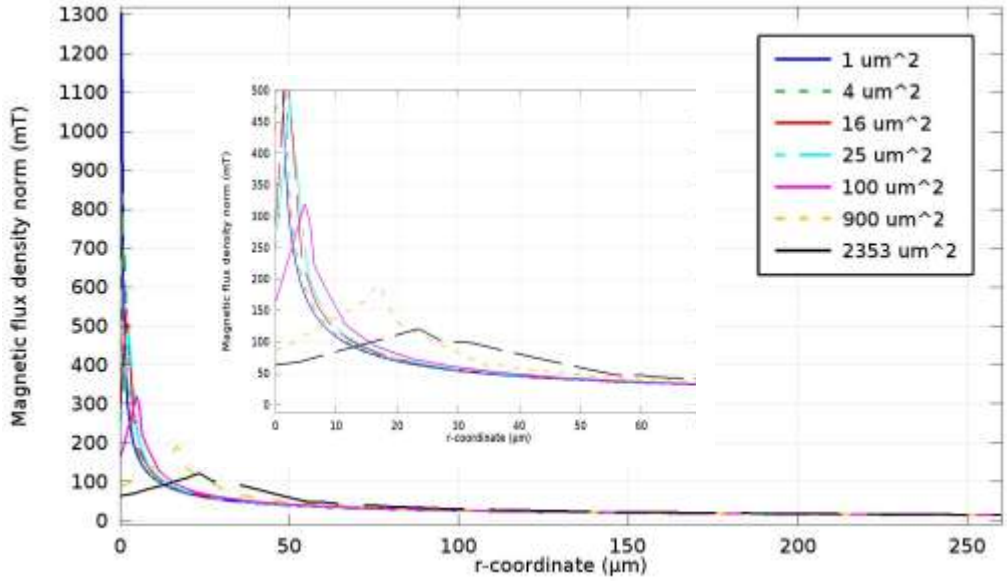


**Figure 6** Normal component of the magnetic flux density, $B_{norm}$, and the gradient profiles for different V-shaped magnetic core tip areas at $I_{dc}$ =3.0 A and z = 0

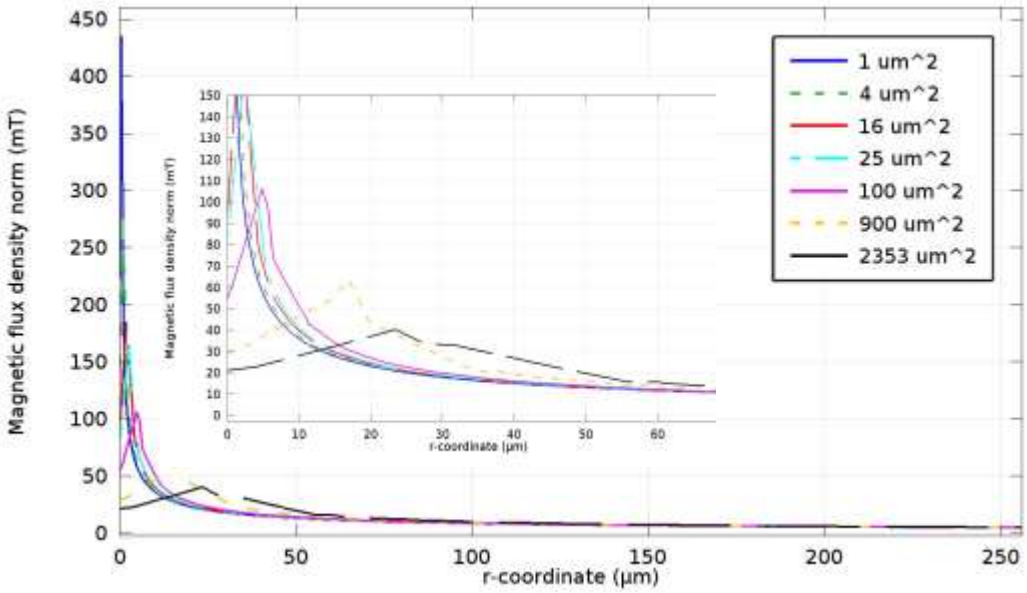


**Figure 7** Normal component of the magnetic flux density, $B_{norm}$, and the gradient profiles for different V-shaped magnetic core tip areas at $I_{dc}$ = 1.0 A and z = 0

As the largest V-shaped area tip of 2353 μm$^2$ was tested for the functional test, further simulation was conducted. Figure 8 shows the effect of current variation on the magnetic flux density generated by the V-shaped area tip of 2353 μm$^2$. The higher the injected current to the microcoils, the greatest the magnetic flux density produced on the core tip, z = 0. The intensification of the magnetic flux density gradient with the current injection was also noticed from the profiles shown in Figure 8, while the calculation is tabulated in Table 3. In this work, the current was limited to 3.0 A due to the possibility of Joule heating effect from the current carrying conductor. The Joule heating effect was undesirable in the LoC separator device as the viability of the biological cells might be endangered. Besides, a considerable drop of magnetic flux density and its gradient with z-coordinate above the core tip is revealed in Figure 9. This result had been as expected and discussed in work of other researchers [12], [13], [21], [22]. Therefore, the proximity distance between the V-shaped core tip to the magnetic nanoparticles suspension was required for greater trapping efficiency.

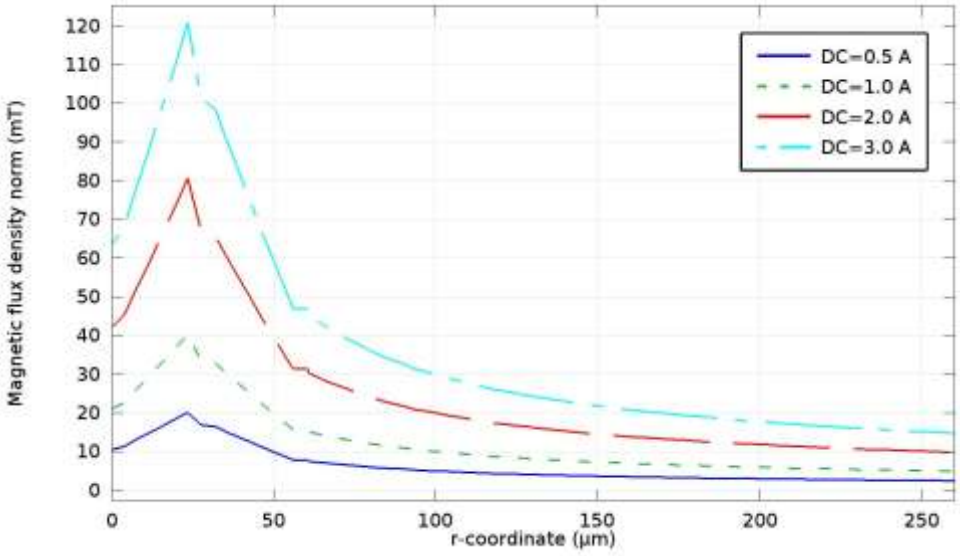


**Figure 8** Normal component of the magnetic flux density, $B_{norm}$, and the gradient profiles for V-shaped magnetic core tip area, 2353 μm$^2$, z = 0 at $I_{dc}$ variation

**Table 3** Maximum magnetic flux density, $B_{norm}$, and its gradient at varying injected current, $I_{dc}$ for A=2353 μm$^2$

| Current $I_{dc}$ (A) | Maximum $B_{norm}$ (mT) | $B_{norm}$ Gradient (T/m) |
|---|---|---|
| 0.5 | 20 | 444.44 |
| 1.0 | 40 | 844.44 |
| 2.0 | 80 | 1733.33 |
| 3.0 | 120 | 2577.78 |

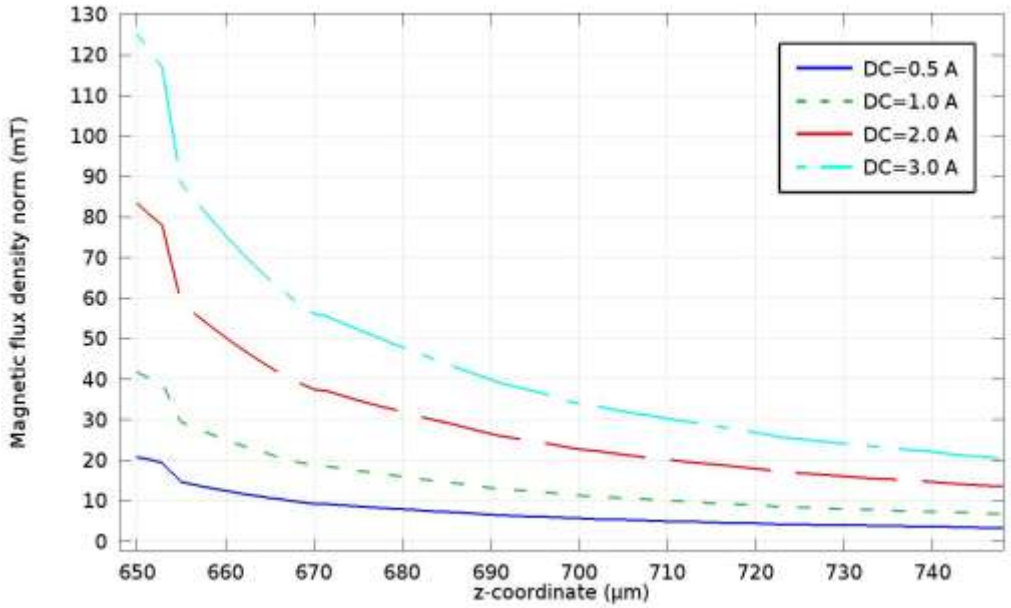


**Figure 9** Normal component of the magnetic flux density, $B_{norm}$, and the gradient profiles for V-shaped magnetic core tip area, 2353 µm² at $I_{dc}$ variation along the z-coordinate above the tip

### 4.3 Effect Of V-Shaped Magnetic Core Tip Area On Magnetic Force On A Nano Sized Particle

In the magnetic separation technique, the most important parameter determined was the magnetic force exerted on the magnetic particles. In this work, Ferrotec Ferrofluids magnetic nanoparticles of 20 nm nominal diameter and initial magnetic susceptibility ~ 5 (SI) had been used as the model. The magnetic force on the 20 nm diameter nanoparticle from V-shaped magnetic core tip area of 2353 $\pi m^2$ was calculated with equation (3) and tabulated in Table 4. A maximum magnetic force of 4.3 x $10^{-16}$ N was developed on a nanoparticle at just above the core tip with $I_{dc}$ of 3.0 A. However, smaller magnetic forces were obtained with low current injection to the microcoils. This result had been expected due to the low magnetic flux density and its gradient values at low current injection.

Effective trapping and sorting of the bioparticles tagged with nanoparticle were justified with high magnetic force, $F_m$, developed on a magnetic nanoparticle in overcoming the drag force experience in the flowing fluid. In a microchannel flow of a big area trapping chamber, the nanoparticle velocity approached zero at the center of the chamber. Therefore, possible trapping was expected with the magnetic force magnitude with higher current injection to the microcoils.

### 4.4 Trapping of 20 nm Nickel Particle at $I_{dc}$ Variation

Experiments were performed by using integrated electromagnet system of magnet wire with spiral-shaped winding, $N$ = 10 turns, and permalloy core tip of area 2353 µm².

**Table 4** Comparison of the magnetic force developed on a 20 nm diameter magnetic particle from 2373 µm² V-shaped magnetic core tip area

| Current, $I_{dc}$ (A) | Magnetic Force, $F_m$ (N) |
|---|---|
| 0.5 | 1.2 x $10^{-17}$ |
| 1.0 | 4.8 x $10^{-17}$ |
| 2.0 | 1.9 x $10^{-16}$ |
| 3.0 | 4.3 x $10^{-16}$ |

The magnetic flux densities generated by the magnet wire were 0.65 mT, 1.29 mT, 2.59 mT, and 3.89 mT at $I_{dc}$ of 0.5 A, 1.0 A, 2.0 A, and 3.0 A respectively. The characterization was performed under static (no flow) fluid condition. Figures 10 (a) to (d) show the nickel nanoparticles trapped at different $I_{dc}$ variations. The images captured by using Analysis software were performed after a 40-second duration of the $I_{dc}$ supplied. For the intended visualization observation, highly concentrated nickel nanoparticles were used. From this experiment, insignificant trapping of the nickel nanoparticles was observed at low $I_{dc}$ supply, i.e. $I_{dc}$ = 0.5 A and $I_{dc}$ = 1.0 A to the magnet system as portrayed in Figures 10 (a) and (b). This had been due to the low magnetic force developed on the nanoparticles. At higher $I_{dc}$ application, the magnetic nanoparticles were trapped as greater trapping area was observed, as shown in Figures 10 (c) and (d), which corresponded to $I_{dc}$ = 2.0 A and $I_{dc}$ = 3.0 A. A dense accumulation of the nanoparticles was observed on the magnetic core tip. During the testing,

movement of the nanoparticles towards the magnetic core tip area was noticed with respect to time. In addition, greater build up area of the trapped magnetic nanoparticles enhanced the magnetic field effects in attracting and trapping other nanoparticles towards the core tip or the sensing zone. The reason for this trapping had been due to the effect of high magnetic nanoparticles permeability in focusing the magnetic flux lines and further enhancing the local magnetic gradient [23]. Besides, the function of the V-shaped magnetic core with micron-sized tip dimension in trapping the magnetic nanoparticles was demonstrated from the testing conducted even at using low magnetic flux density source from coil winding magnetic wire.

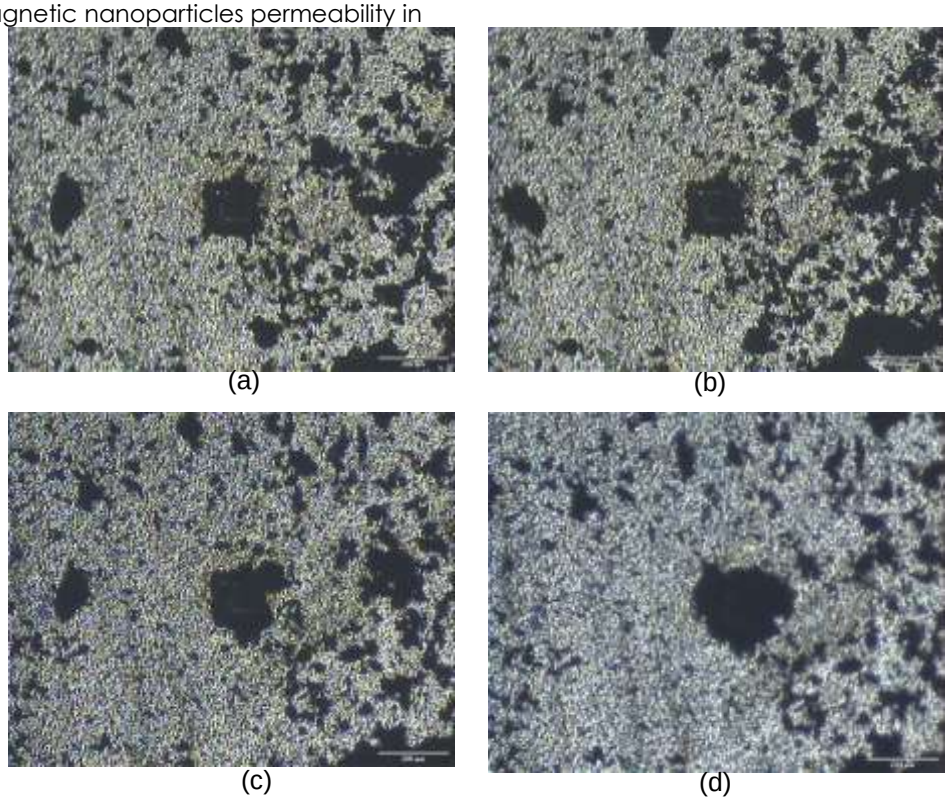


**Figure 10** Nickel magnetic nanoparticles trapped after 40 seconds at (a) $I_{dc}$ = 0.5 A (b) $I_{dc}$ = 1.0 A (c) $I_{dc}$ = 2.0 A and (d) $I_{dc}$ = 3.0 A

## 5.0 CONCLUSION

In this work, high magnetic flux density and gradient magnetic system were designed to be part of LoC magnetic separator. The proposed design is considered as a new innovation for high magnetic gradient generation due to the exploitation of the V-shaped permalloy magnetic core as the magnetic flux lines guider and concentrator. In addition, the effects of V-shaped magnetic core tip area and the current injection on the magnetic flux density, as well as its density, had been simulated and studied. It can be concluded that the smallest V-shaped magnetic core tip area and the highest current injected to the microcoils had significantly amplified the magnetic flux density, its gradient, and the magnetic force developed on a nanoparticle. Besides, magnetic nanoparticles trapped using the fabricated magnetic core of micron-sized tip and magnetic field source from spiral winding magnet wire was also conducted as a proof of concept test. Greater trapping area that resulted from the nanoparticles accumulation at the magnetic core tip was observed at high current injection to the magnet wire. Therefore, the potential of V-shaped magnetic core to be part of the integrated LoC magnetic separator device, as proposed in this work, had been justified.

## Acknowledgement

We are grateful for the UTM scholarship to Author 1 and we would like to thank the Malaysian Ministry of Higher Education and Universiti Kebangsaan Malaysia for the research grant under project NND/ND/(1)/TD11-002.

## References

[1] Lim, Y. C., Kouzani, A. Z. and Duan, W. 2010. Lab-on-a-chip: a Component View. *Microsystem Technologies*. 16 (12): 1995–2015

[2] Ganguly, R. and Puri, I. K. 2010. Microfluidic Transport in Magnetic MEMS and BioMEMS. *Wiley Interdisciplinary Reviews. Nanomedicine Nanobiotechnology*. 2(4): 382–99
[3] Pankhurst, Q. A., Connolly, J., Jones, S. K. and Dobson, J. 2003. Applications of Magnetic Nanoparticles in Biomedicine. *Journal of Physics. D. Applied Physics.* 36 (13): R167–R181
[4] Cao, Q., Han, X. and Li, L. 2014. Configurations and Control of Magnetic Fields for Manipulating Magnetic Particles in Microfluidic Applications: Magnet Systems and Manipulation Mechanisms. *Lab Chip*. 14(15): 2762–77
[5] Ramadan, Q., Samper, V., Poenar, D. P. and Yu, C. 2006. An Integrated Microfluidic Platform for Magnetic Microbeads Separation and Confinement. *Biosensors Bioelectronics*. 21 (9): 1693–702
[6] Ramadan, Q., Samper, V. D., Puiu, D. P. and Yu, C. 2006. Fabrication of Three-Dimensional Magnetic Microdevices With Embedded Microcoils for Magnetic Potential Concentration. *Journal Microelectromechanical Systems.* 15 (3): 624–638
[7] Smistrup, K., Tang, P. T., Hansen, O. and Hansen, M. F. 2006. Microelectromagnet for Magnetic Manipulation in Lab-on-a-chip Systems. *Journal of Magnetism and Magnetic Materials*. 300 (2): 418–426
[8] Inglis, D. W., Riehn, R., Sturm, J. C. and Austin, R. H. 2006. Microfluidic High Gradient Magnetic Cell Separation. *Journal of Applied Physics*. 99 (8): 08K101
[9] Kong, H. S. E, Sugiarto, H. S., Liew, H. F., Wang, X., Lew, W. S., Nguyen, N.-T. and Chen, Y. 2010. An Efficient Microfluidic Sorter: Implementation of Double Meandering Micro Striplines for Magnetic Particles Switching. *Microfluid Nanofluidics*. 10 (5): 1069–1078
[10] Fulcrand, R., Jugieu, D., Escriba, C., Bancaud, A., Bourrier, D., Boukabache, A. and Gué, A.M. 2009. Development of a Flexible Microfluidic System Integrating Magnetic Micro-actuators for Trapping Biological Species. *Journal of Micromechanics Microengineering*. 19(10): 105019
[11] Dong, T., Su, Q., Yang, Z., Karlsen, F., Jakobsen, H., Egeland, E. B. and Hjelseth, S. 2010. Fully Integrated Micro-Separator with Soft-Magnetic Micro-pillar Arrays for Filtrating Lymphocytes. *Conference Proceeding of IEEE Engineering Medical Biology Society*. Buenos Aires, Argentina. 6522–6526
[12] Ramadan, Q., Poenar, D. P. and Yu, C. 2008. Customized Trapping of Magnetic Particles. *Microfluid. Nanofluidics*. 6 (1): 53–62
[13] Xia, N. , Hunt, T. P., Mayers, B. T., Alsberg, E., Whitesides, G. M., Westervelt, R. M. and Ingber, D. E. 2006. Combined Microfluidic-micromagnetic Separation of Living Cells in Continuous Flow. *Biomedical Microdevices.* 8(4): 299–308
[14] Yapici, M. K. and Zou, J. 2008. Permalloy-coated Tungsten Probe for Magnetic Manipulation of Micro Droplets. *Microsystem Technologies*. 14(6): 881–891
[15] Barbic, M., Mock, J. J., Gray, A. P. and Schultz, S. 2001. Scanning Probe Electromagnetic Tweezers. *Applied Physics Letters.* 79. (12): 1897
[16] Matthews, B. D., LaVan, D. a., Overby, D. R., Karavitis, J. and Ingber, D. E. 2004. Electromagnetic Needles with Submicron Pole Tip Radii for Nanomanipulation of Biomolecules and Living Cells. *Applied Physics Letters.* 85(14): 2968
[17] Pamme, N., Eijkel, J. C. T. and Manz, A. 2006. On-chip Free-flow Magnetophoresis: Separation and Detection of Mixtures of Magnetic Particles in Continuous Flow. *Journal of Magnetism Magnetic Materials*. 307(2): 237–244
[18] Pamme, N. 2006. Magnetism and Microfluidics. *Lab Chip.* 6 (1): 24–38
[19] Shafique M. and Hansen, M. F. 2003. Modeling the Magnetic Field From a Microelectromagnet in FEMLAB. *Proceedings from the Nordic MATLAB Conference*. Copenhagen, Denmark. 209–214
[20] COMSOL. *Introduction to ACDC Module*. 2014
[21] de Vries, A. H. B., Krenn, B. E., van Driel, R. and Kanger, J. S. 2005. Micro Magnetic Tweezers for Nanomanipulation Inside Live Cells. *Biophysics Journal*. 88(3): 2137–44
[22] Fulcrand, R., Bancaud, A., Escriba, C., He, Q., Charlot, S., Boukabache, A. and Gué, A.-M. 2011. On chip Magnetic Actuator for Batch-mode Dynamic Manipulation of Magnetic Particles in Compact Lab-on-chip. *Sensors Actuators B Chemicals*. 160(1):1520–1528,
[23] Teste, B., Malloggi, F., Gassner, A.-L., Georgelin, T., Siaugue, J.-M., Varenne, A., Girault, H. and Descroix, S. 2011. Magnetic Core Shell Nanoparticles Trapping in a Microdevice Generating High Magnetic Gradient. *Lab Chip.* 11(5): 833–4